Designing for Conductor Lay and AC Loss Variability in Multistrand Stator Windings

Hoole, J., Mellor, P. H., Simpson N.

ACCEPTED PAPER

To be published in the IEEE Transactions on Industry Applications

DOI: 10.1109/TIA.2022.3202762

Designing for Conductor Lay and AC Loss Variability in Multistrand Stator Windings

Joshua Hoole, Philip H. Mellor, *Member, IEEE,* and Nick Simpson, *Member, IEEE*

***Abstract*—Vehicle electrification places significant pressures on electric machine design due to the need for increased power densities and mass production. These two requirements couple when designing multistrand stator windings, which exhibit significant AC loss variability as a result of the random nature of the conductor lay within the stator slot caused by automated insert winding. This paper presents two prediction methods for AC loss variability to be deployed at the winding design stage. The first consists of an analytical approach, whilst the second constructs a 2D finite element analysis geometry that captures conductor lay characteristics. Comparison of predictions from both approaches to experimental AC loss measurements established that the proposed models capture the experimentally observed AC loss variability characteristics and that the analytical method is suitable for early design stages whilst the finite element approach should be adopted once the winding configuration is finalised.**

***Index Terms*—AC loss, high frequency, electrical machine windings, loss and thermal modelling, statistical variation**

I. Introduction

THE advance towards net-zero carbon targets places unique pressures on the adoption of electric traction motors within the automotive sector. Electrical machines in such applications must demonstrate high power density and high efficiencies to meet the range specifications demanded for electric vehicles [1]. To achieve high power densities, winding AC excitation frequencies in excess of 1 kHz are now common [2], leading to significant winding eddy current loss. The volume manufacture of these windings often necessitates the adoption of multistrand bundles composed of multiple small diameter parallel 'strands-in-hand' to mitigate skin effect losses (see Fig. 1a) [3]. However, such winding configurations are susceptible to inter-strand circulating currents that cause bundle-level losses [4]. These AC losses can be a major component of stator loss, impacting the thermal rating and efficiency of power dense electrical machines [5].

A further challenge imposed upon electric vehicle traction motors is that the mass production manufacture used to reduce cost can restrict the choice of winding format. The manufacture of multistrand windings is reliant on the automated insert winding process, a comprehensive description of which is provided by Hagedorn et al. [6]. A flyer is used to form air coils consisting of the parallel strands-in-hand, with consecutive series turns being stacked upon one another [7], [8]. Insertion tooling then draws the coils into the stator slots [7], [8]. Due to the large number of physical interactions between strands, coils and tooling, significant conductor transposition occurs, resulting in mixing of conductor strands within and between series turns in a coil. The insert winding process also prevents the use of Litz wire due to the potential for the strand insulation to be damaged during manufacture [9].

J. Hoole, P. H. Mellor and N. Simpson are with the Electrical Energy Management Group, University of Bristol, Bristol, BS8 1TR, United Kingdom email: josh.hoole@bristol.ac.uk

Manuscript received May 2022, Revised July 2022

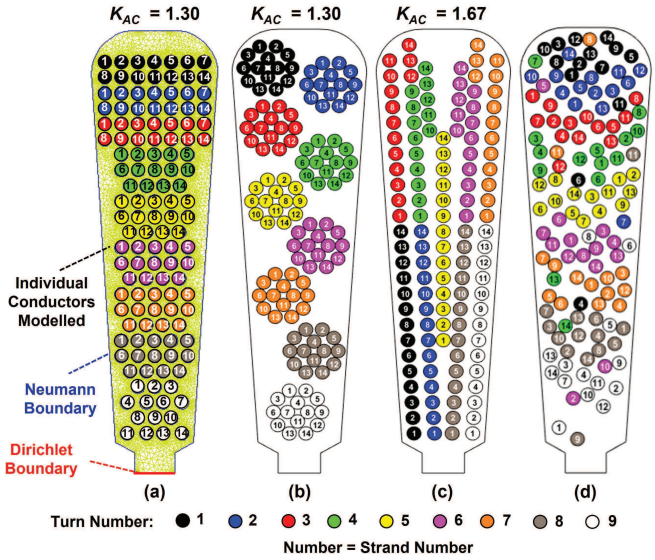

Fig. 1. 2D AC harmonic FEA model for AC loss estimation model when assuming (a) tangential, (b) bundle, (c) radial and (d) random conductor lays

The automated winding process ultimately results in variability in the conductor lay, specifically where the individual series turns that form the parallel connected bundle strands sit within the stator slot [8], [10], [11]. The layered multistranded winding of 9 turns of 14 parallel 'strands-in-hand' shown in Fig. 1a would therefore be very challenging to achieve in practice and the likely conductor lay would be more akin to Fig. 1d, where the strands forming the bundle turns are more randomly mixed [12]. Further, strand transposition has been observed throughout the winding, with strands weaving along the slot active length and end winding [13]. Consequently, manufacturing processes lead to a conductor lay and strand positioning that varies from slot-to-slot and stator-to-stator, also known as a 'random winding' [4]. Previous studies have highlighted how the geometric positioning of conductors can have a profound influence on the AC loss magnitude [3], [10], [11]. This important early work has focused on understanding the potential range of the AC loss variations in considering bounding and idealised conductor lays, such as the tangential and radial arrangements shown in Fig. 1a and 1c respectively.

However, as the AC loss effect is sensitive to the position of specific conductors, significant variability occurs in the AC losses of as-manufactured windings [3], [14]. Due to the loss variability across a production batch, some stators may demonstrate localised hot-spots and premature in-service failure, with added costs in increased inspection, high reject rates, or derating to accommodate the outlier spread in variance [14].

There have been previous efforts to simulate the variability in the conductor lay and strand positions [4], [12], [15], [16] and this paper extends this prior work by developing computationally efficient analysis tools that characterise AC loss variability with a view to supporting the design of random multistranded windings in power-dense electrical machines. The tools consist of experimentally-informed analytical and Finite Element Analysis (FEA) methods. By accounting for conductor lay variability at the design stage, the AC loss variability can be characterised, leading to an assessment of the winding reliability in-service. This ultimately reduces design cost and risk, whilst also supporting winding configuration optimisation [14]. The ultimate aim of this paper is to establish recommendations for the utilisation and future development of analysis approaches to support the characterisation of AC loss variability during electrical machine design.

II. Experimental AC Loss Estimation

AC losses within multistrand windings can be decomposed into two levels, *strand* and *bundle* losses [15], [17]. Strand-level losses arise from the current crowding towards the surface of a conductor at high excitation frequencies [18] and proximity losses resulting from fields external to the conductor, such as the slot leakage flux arising from neighbouring conductors and rotor induced fields [15]. Bundle losses are the result of circulating currents within the multiple parallel strands that form each series turn and occur as a result of imbalances in the induced voltages and impedance of each strand circuit [15], [17]. Bundle level losses are sensitive to the different conductor positions that a parallel strand occupies in a stator slot [12]. Combined, the magnitude of strand and bundle losses within a stator winding are often defined using the 'AC loss factor' K_{AC}, which represents the ratio of the AC to DC ohmic power loss at a given frequency and temperature. Whilst core losses can also be significant at high AC excitation frequencies, in modern electric vehicle traction motors core losses are a small proportion of the total machine loss when compared to winding copper losses due to the use of advanced electrical steels and thin laminations [19], [20].

A common approach to generating AC loss characteristics for a given winding configuration is to perform AC loss testing of winding sub-assemblies ('motorettes') [3], [21], prototype windings [22], or even full machines [4], [10]. Repeated testing of different windings from the same production batch can be used to estimate the AC loss variability resulting from the variable conductor lays as a result of the manufacturing process. Such an approach was adopted by Preci et al. [14]. The current paper extends this prior work by characterising how frequency and temperature impact AC loss variability.

The initial characterisation of AC loss variability was performed using experimental measurements of AC loss from a batch of random distributed wound 3-ph 4-pole induction motor stators. The rotors of three induction machines were removed, facilitating the AC loss measurements of 9 individual phase windings (i.e. 3 stators with 3 phase windings each).

A California Instruments CSW AC source was used to generate a current-controlled (1A) AC supply to an individual phase winding, whilst the supply frequency was swept from f = 40Hz to f = 1.5 kHz, during which the power consumption of the single phase winding was recorded using a Fluke Norma power analyser. The K_{AC} at each point in the frequency sweep could be estimated using the recorded power values and winding DC loss at the test temperature. The AC loss measurements were conducted in a TAS Environmental Chamber to permit the winding operating temperature to be varied. The employed experimental setup is shown in Fig. 2. The AC loss measurements across the frequency sweep were repeated for each available phase winding at 25°C, 50°C, 75°C, 100°C and 125°C. K-type thermocouples, inserted into a stator slot and an end winding (see Fig. 2) monitored the winding temperature.

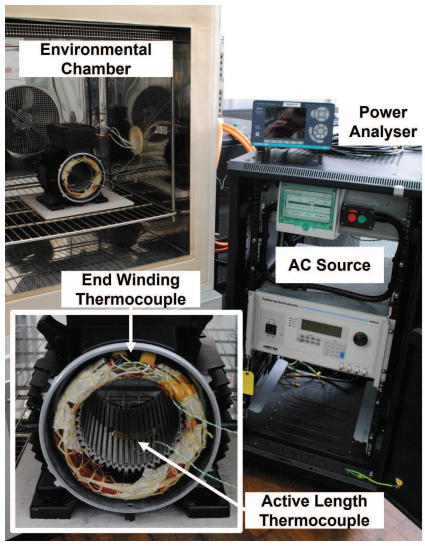

Fig. 2. The experimental set up for measuring phase winding AC loss

A. Mean AC Loss Behaviour

In order to characterise the AC loss behaviour of the phase windings with respect to AC excitation frequency f and temperature T, the mean K_{AC} value across the 9 phase windings was computed at each test point as given in Fig. 3, which shows that K_{AC} increases with frequency as anticipated [23]. The mean K_{AC} can also be seen to reduce with increasing temperature, consistent with previous work [24]. A reduction in K_{AC} with increasing temperature is to be expected, due to the increase in resistivity, leading to an increase in the winding DC ohmic loss and a reduction in the circulating current losses [23]. With increasing resistivity, the conductor skin depth also increases, further reducing AC losses.

B. AC Loss Variability Behaviour

The AC loss measurements across 9 phase windings permitted K_{AC} variability characterisation. Fig. 4 shows the variability in K_{AC} as a histogram at T = 25°C and f = 1.5 kHz, with a corresponding coefficient of variation (the sample standard deviation of K_{AC} divided by its mean value, expressed as a percentage) of $c_v = 1.50\%$. It is important to reiterate that the variability shown in Fig. 4 is due to different conductor lays present in each of the 9 phase windings and hence different AC loss values for each test winding, rather than measurement error on repeated tests of a single winding.

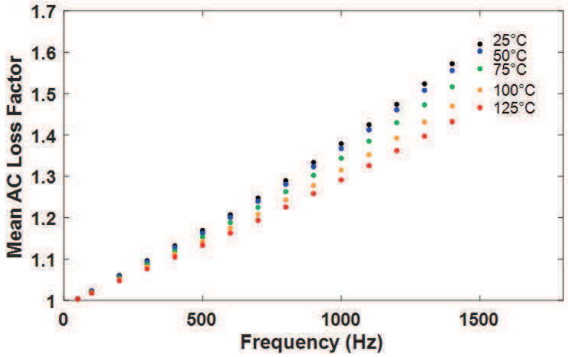

Fig. 3. Mean phase winding AC loss factor at varying temperature and frequencies

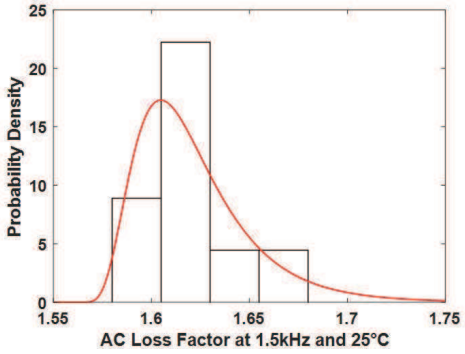

Fig. 4. The variability in AC loss factor at 1.5 kHz and 25°C as characterised using a 3P Log-Normal distribution

The variability shown in Fig. 4 was further characterised by fitting a 3P Log-Normal distribution and full justification for selecting a 3P Log-Normal distribution is provided in previous work [12]. A 3P Log-Normal distribution has the form shown in (1), where x is the value of the quantity of interest (i.e. K_{AC}), $p(x)$ is the probability density, δ_{LN} is a threshold parameter (minimum possible value), μ_{LN} is a location parameter (representative of distribution 'peak' position) and σ_{LN} is a scale parameter (representative of the distribution 'spread') [12]. Fig. 4 shows a 3P Log-Normal distribution fitted to the K_{AC} variability at T = 25°C and f = 1.5 kHz and an good fit to the histogram can be observed.

$$p(x) = \frac{1}{\sigma_{LN}(x-\delta_{LN})\sqrt{2\pi}} exp\left(-\frac{(ln(x-\delta_{LN})-\mu_{LN})^2}{2\sigma_{LN}^2}\right) \quad (1)$$

Across the remaining test points, the K_{AC} variability was characterised using a 3P Log-Normal distribution along with c_v values and Table I shows the resulting 5th (5prc) and 95th (95prc) percentiles, along with the Inter-Percentile Range (IPR), which is the difference between the 95prc and 5prc values. It can be observed that variability increases with increasing frequency (due to the increasing IPR value), as also shown in Fig. 5a and the increasing c_v value with respect to frequency at T = 25°C (see Fig. 5b). As the magnitude of AC loss increases with frequency, and is sensitive to the variability in the conductor lay, it should be anticipated that AC loss variability will increase with increasing frequency.

TABLE I
AC LOSS VARIABILITY AS CHARACTERISED USING 3P LOG-NORMAL DISTRIBUTIONS

f (kHz)	K_{AC} at 50°C			K_{AC} at 125°C		
	5prc	95prc	IPR	5prc	95prc	IPR
0.5	1.158	1.173	0.015	1.129	1.141	0.012
1.0	1.356	1.399	0.043	1.283	1.306	0.023
1.5	1.583	1.653	0.070	1.449	1.486	0.037

Table I also highlights that the variability in AC loss reduces with increasing temperature, as shown by the reducing IPR value at a given frequency. In some instances, it can be observed that the highest performing machines have AC loss magnitudes similar to the lowest performing machines at the next increase in temperature by 25°C, as shown in Fig. 5c. The reduction in AC loss variability with increasing temperature is also visualised in Figs. 5c and 5d by the K_{AC} distributions and reducing c_v value with increasing temperature. Again, as the mean K_{AC} reduces with increasing temperature, a reduction in the AC loss variability with increasing temperature should also be expected. The plateau observed within the AC loss variability is as a result of the proportion of AC losses related to the bundle effect reducing with increasing temperature.

III. AC Loss Estimation via Analytical Approach

Naturally, during winding design, methods are required to produce AC loss estimates prior to the construction of physical prototypes, which require extensive resources and time for manufacture and testing, especially when considering variability or various candidate winding designs [25].

Analytical methods are often employed for AC loss estimation, due to their reduced computational expense compared to electromagnetic FEA-based approaches [26]. Simplified models are valuable at a system level in estimating the loss behaviour of an electrical machine across its operating envelope. A large number of analytical methods have been presented in the literature [17], [26]–[28]. However, analytical methods are often constructed for a defined conductor lay (e.g. Litz transposition [17]) and therefore can be inaccurate when applied to other conductor lay arrangements [26]. Consequently, analytical methods can be challenging to generalise

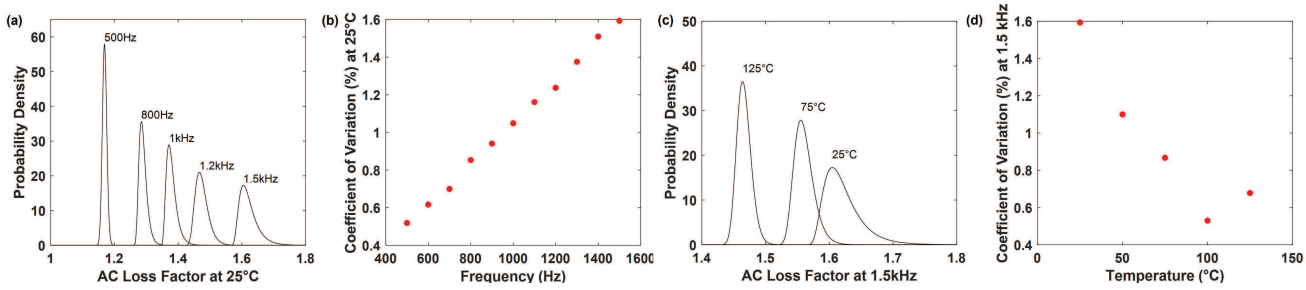

Fig. 5. (a) 3P Log-Normal Distributions and (b) coefficient of variation for AC loss factor at different frequencies at 25°C. (c) 3P Log-Normal Distributions and (d) coefficient of variation for AC loss factor at different temperatures at 1.5 kHz

for a new winding configuration and slot geometry, and also currently fail to characterise AC loss variability. A behavioural model for AC loss variability has been presented by the authors [15]. The total AC loss factor K_{AC} is separated into strand and bundle AC loss components, K_{ACs} and K_{ACb} respectively.

$$K_{AC} = 1 + K_{ACs} + K_{ACb} \tag{2}$$

Strand AC loss is determined using published methods drawing from the work of Sullivan [29], which assumes the conductor dimension is sufficiently small to behave as a resistance limited problem. In this case, the strand loss varies with operating frequency, f and conductor temperature T, and can be approximated using (3) and (4). K_{ACs0} is the strand AC loss evaluated at a representative base operating frequency f_0 and temperature T_0 and is determined from a knowledge of the winding conductor diameter and geometric design; α_T is the temperature coefficient of resistivity of the wire used. The f_c term represents the scaled base operating frequency with respect to temperature and provides a mathematically convenient way to permit the analytical model to be applied to varying frequencies and temperatures simultaneously.

$$K_{ACs} = K_{ACs0}\left(\frac{f}{f_c}\right)^2 \tag{3}$$

$$f_c = f_0(1 + \alpha_T(T - T_0)) \tag{4}$$

A behavioural model that provides a good estimate for the bundle AC loss factor, K_{ACb} in a random lay multistranded winding is given in (5). The model has been derived considering the circuit behaviour of parallel connected strands based on the following simplifying assumptions [15]:

- The bundle AC loss factor is not dependent on the operating phase current magnitude, I_p, or the current angle. Saturation effects are thus neglected.
- The effect of the winding lay is modelled as a statistical variance in the AC loss factor by a probability distribution (e.g., Normal $N(1, \sigma)$). The shape (variance) of this distribution is independent of frequency and temperature.
- Bundle AC loss variation is driven from the active slot region with the end winding approximated as a fixed per strand inductance independent of the conductor lay.

Winding design specific parameters K_{ACb0}, f_0 and σ are found from a 2D slot based harmonic FEA or analytical field solution using a randomized algorithm to determine conductor placement and how conductors are grouped to form each in-hand bundle [15]. Fig. 6 indicates the fit of (5) to the mean AC loss predictions across various operating frequencies and temperatures, suggesting it captures the trends well [15].

$$K_{ACb} \cong 2K_{ACb0}\frac{\left(\frac{f}{f_C}\right)^2}{1 + \left(\frac{f}{f_c}\right)^2}N(1, \sigma) \tag{5}$$

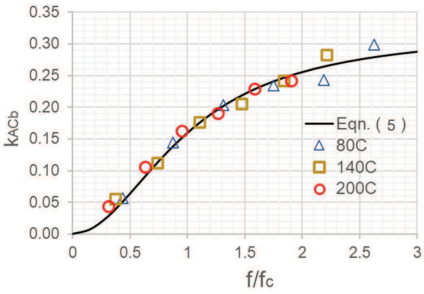

Fig. 6. Fit of AC loss model (5) to simulated AC loss data [15]

A. Calibration of Analytical Approach to Experimental Data

The analytical behavioural model could be fitted via least squares to the mean experimental K_{AC} values. It was observed that the model resulted in a reduced fit at $T = 25°C$, and consequently the model was only fitted to the experimental data at 50°C, 75°C, 100°C and 125°C. The reduced fit of the analytical model at 25°C will be discussed in Section V. At a reference temperature of $T_0 = 50°C$, the corner frequency $f_c = 420$ Hz, $K_{ACs0} = 0.033$ and $K_{ACb0} = 0.11$, suggesting that bundle losses represent the most significant component of AC loss. Fig. 7 shows good agreement between the predicted mean K_{AC} values from the analytical model and those observed across the 9 tested phase windings at various operating frequencies and temperatures.

When comparing the bundle losses derived from (5) to the experimental AC loss variability, it was observed that the K_{AC} variability failed to decrease with increasing temperature and that the skewed behaviour of the 3P Log-Normal distribution for K_{AC} variability was not captured. Consequently, (5) was modified to apply a Log-Normal distribution to K_{ACb}, as shown in (6), where LN represents a 2-Parameter Log-Normal

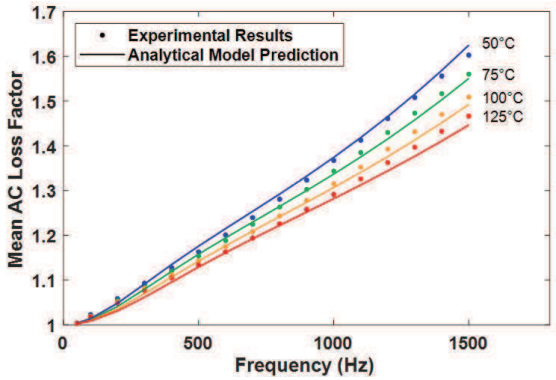

Fig. 7. Comparison between mean AC loss values predicted by the analytical AC loss model and the experimentally derived mean AC loss values

distribution, defined using a mean of $m = 1$ and a variance of v, which is scaled by the frequency temperature correction. The Log-Normal distribution parameters, μ_{LN} and σ_{LN}, can be derived from m and v using standard equations [12].

$$K_{ACb} \cong 2K_{ACb0}\frac{\left(\frac{f}{f_c}\right)^2}{1+\left(\frac{f}{f_c}\right)^2} LN\left(1, v\left(\frac{f}{f_c}\right)^2\right) \qquad (6)$$

The value of v is defined via least squares fit to minimise the error from the IPR values shown previously in Table I, through computing the estimated 5$^{\text{th}}$ and 95$^{\text{th}}$ percentiles of the predicted K_{AC} values. The least squares fit resulted in $v = 5.5 \times 10^{-3}$ and Fig. 8 compares the predicted K_{AC} variability with the variability observed during experimental testing, with good agreement in IPR values observed. Fig. 8 shows that (6) captures the experimentally observed AC loss variability behaviour, of increasing variability with increasing frequency at a given temperature, and decreasing variability with increasing temperature at a given frequency.

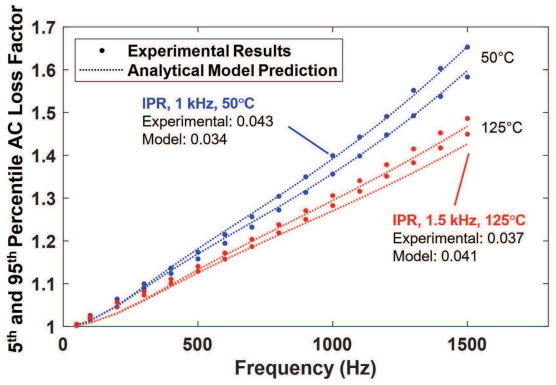

Fig. 8. AC loss variability behaviour as predicted by the analytical model

IV. FEA: Statistical Simulation Methodology

The alternative to analytical approaches to AC loss estimation is the adoption of electromagnetic FEA models [3], [12]. FEA approaches can be generalised to any slot geometry, winding configuration and assumed 'conductor lay' (i.e. cross-section and position of the winding within the slot, and the position of each conductor) and 'strand assignment' (i.e. the conductor positions that each parallel strand occupies across its turns) [30]. A significant proportion of the literature is dedicated to FEA models, typically consisting of 2D FEA models (see Fig. 1a) which model each individual conductor as a homogeneous current carrying region, with external circuit models being used to represent the parallel connected strands [3], [12], [15]. The surrounding iron is assumed to be ideal, with semi-closed slots mitigating the flux penetration from the rotor (wide slots can also be accounted for [15]). 2D FEA dominates current practice, with 3D FEA only being used for concentrated windings [31], [32] and assessing end winding effects [33]–[35] due to the significant computational resource required. Hybrid analytical-FEA approaches have also been proposed to minimize the computational burden [5], [30].

The variability in the position of each turn of each parallel strand within the stator slot can be decomposed into the conductor lay and strand assignment. The historical lack of data regarding the conductor lay and strand assignment in as-manufactured windings requires significant assumptions to be made when constructing AC loss models. A review of the literature highlights that 'tangential' [3], [10], [11], [21], [26], [36]–[40], 'radial' [1], [3], [10], [11], [21], [26], [36], [38]–[40] and 'bundle' [1], [3], [9], [11], [21], [26], [39], [41]–[44] are commonly-assumed strand assignments as visualised in Fig. 1 along with their corresponding K_{AC} values (as computed using 2D FEA). It can be observed that there is nearly a 30% difference in the minimum and maximum K_{AC} values for the tangential and radial arrangements respectively.

A recent focus has been the development of methods to capture the variability in conductor lays and strand assignments, to facilitate a departure from the assumed arrangements in the literature. Lehikoinen et al. have presented a methodology that randomly swaps individual elements of the strand assignment [4], [45]. Chai et al. have presented a methodology where the strands are randomly assigned to the assumed conductor lay [36]. Efforts have also been made to simulate the conductor lay (i.e. position of conductors in the slot) by Hoffmann et al. [16], Du-Bar and Wallmark [46] along with Veg et al. [47]. Beyond AC loss estimation, such methodologies have also been used for assessing thermal performance [47], voltage stresses [16] and to benchmark new winding technologies [31], [46].

A. Observed Conductor Lay Characteristics

Random winding conductor lay characteristics have been characterised using visual inspection [45], sectioning of windings [16], [41], colouring of conductors [48] and using X-ray [13], [49]. Firstly, ground wall insulation, slot liners and slot wedges have been observed to lead to the triangular and rounded conductor formations at the slot opening and slot back respectively [13], [16], [41], [45]. The triangular formation of conductors is important to represent at the slot opening, due to the significant sensitivity of AC losses to the proximity and arrangement of conductors at the slot opening [3], [11].

Irregular edges of the winding cross-section and gaps within the conductor lay have been previously observed via X-ray and

in sectioned machines [13], [16], [41]. The formation of irregular winding edges and gaps within the winding cross-section is expected to occur due to the conductors being 'dragged' against the slot wall during coil insertion into the stator. As deviation away from a regular conductor lay will alter the conductor proximity and bundle losses, such characteristics must be incorporated into conductor lay simulations

Finally, X-ray has shown that both the position of the winding cross-section within the stator slot, along with the proximity of conductors to the slot opening is highly variable, as shown in Fig. 9 [13]. In a similar manner to replicating triangular conductor formations at the slot opening, the variability in the proximity of conductors to the slot opening should also be accounted for in simulations to permit an accurate estimation of the AC loss variability [11], [39], [44].

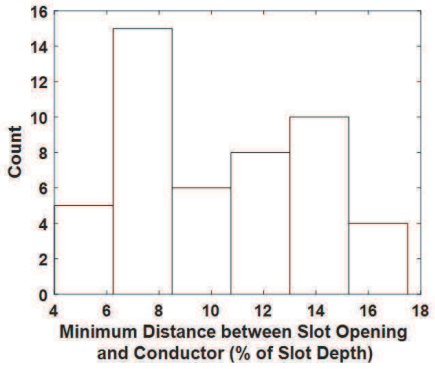

Fig. 9. Variability in closest position of conductor to slot opening [13]

B. Modelling of Conductor Lay Characteristics

The development of a Statistical Simulation Methodology (SSM) is reliant on exploiting the ability of 2D FEA models to represent the position and strand assignment of individual conductors. This section aims to build upon the prior work of the authors [12] to develop an SSM that captures observed conductor lay characteristics. Within the SSM, the regular and fixed conductor grid was modified from that in Fig. 1a to incorporate a triangular conductor lay at the slot opening and a rounded lay at the slot back (see Fig. 10a).

To represent the irregular edges to the winding cross-section, the alternating conductors per layer in the fixed grid previously defined in Fig. 1a was retained. By over-specifying the number of conductors within the lay, individual conductors were selected at random to be removed, leading to irregular edges and gaps within the winding cross-section (see Fig. 10a).

Finally, to capture the varying position of the winding cross-section within the stator slot, along with the varying proximity of conductors towards the slot opening, the entire simulated conductor lay could be shifted along the slot depth direction (see Fig. 10b and 10c). This was achieved by histogram sampling of the data shown previously in Fig. 9, to achieve the required variability in conductor proximity to the slot opening.

C. Modelling of Strand Assignment Variability

The SSM must also be capable of representing the variation in the strand assignment within the winding. An initial investigation was performed for a winding configuration of 9 turns of 14 'strands-in-hand' (see Fig. 10). To enable comparison with previous results, the AC excitation frequency was set to f = 1.5 kHz at a temperature of T = 25°C. A Monte Carlo Simulation (MCS) was employed for 10,000 iterations (a typical MCS benchmark [4]) and for each iteration a new conductor lay and a random strand assignment was generated and the resulting 2D FEA model executed. When parallelised over four computer cores (3.40 GHz, 16.0 GB RAM), it was found that each iteration required approximately 3.5 seconds to perform both the lay simulation and the subsequent FEA.

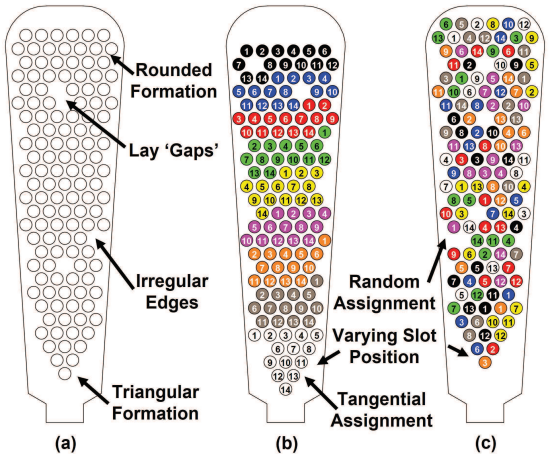

Fig. 10. (a) the simulated conductor lay, (b) a tangential strand assignment and (c) a random strand assignment

A further MCS was performed which assumed a tangential strand assignment for every generated conductor lay. The assumption of a tangential assignment would therefore represent the variability in K_{AC} arising solely from conductor lay variability. Examples of simulated conductor lays and strand assignments are shown in Fig. 10b and 10c.

The resulting K_{AC} variability in the form of fitted 3P Log-Normal distributions are shown in Fig. 11. Qualitatively, it can be observed that the introduction of a random strand assignment significantly increases the variability in K_{AC}, whilst also reducing the positive skew observed in the distribution.

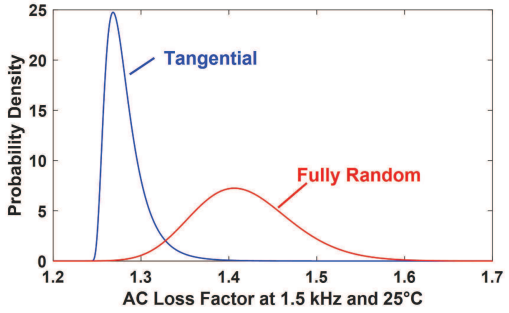

Fig. 11. The variability in AC loss factor across 10,000 MCS iterations for the simulated conductor lay with tangential and purely random strand assignments

In order to compare the variability characteristics between the FEA models and the experimental results shown in Section

II, the 3P Log-Normal distributions were translated by each distribution $-\delta_{LN}$ value, as shown in Fig. 12. Such a translation is required to remove dependency on AC loss magnitude, resulting from the differing winding configurations, and hence K_{AC} magnitude, between the tested phase windings and FEA model. This translation shifts the entire distribution shape left along the x-axis, and as δ_{LN} is a threshold, the translation aligns the distributions to start at the same zero location.

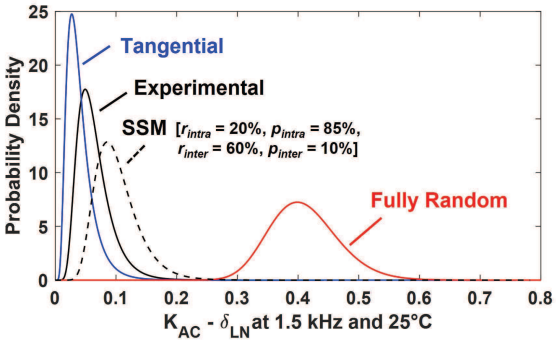

Fig. 12. The collapsed and translated distributions for AC loss factor variability as characterised from tangential and purely random strand assignments, along with the experimental results from Section II and the authors' previous statistical simulation methodology [12]

From Fig. 12, it can be seen that the translated distribution for the experimental K_{AC} lies between those of the tangential and fully random strand assignments. It was hypothesised that as the level of strand deviation from the tangential arrangement increases, AC loss variability will tend towards the experimentally observed characteristics. Fig. 12 also suggests that the resulting strand assignments will be similar to a tangential arrangement, as the experimentally-derived distribution is significantly closer to the tangential K_{AC} distribution shape.

In order to calibrate the SSM strand assignment, an approach similar to that presented previously by the authors was employed [12]. However, it is important to note that this previous methodology does not adequately capture the conductor lay characteristics identified in Section IV-A. Therefore, the starting point for the strand assignment was the generation of a conductor lay (see Section IV-B) and a tangential strand assignment as shown in Fig. 13a and 13b respectively.

The SSM randomly swaps the strand assignment within each series turn (i.e. *intra-turn*) as shown in Fig. 13c. A swap takes place if the randomly selected position to swap is within a specified radius r_{intra} (expressed as a percentage of slot depth) with a probability of a swap occurring p_{intra}. Strand assignment swaps between each series turn (i.e. *inter-turn*) are also performed, defined by maximum radius r_{inter} and a swap probability p_{inter} (see Fig. 13d). A 100 iteration MCS was performed employing values previously defined in [12], where r_{intra} = 20%, p_{intra} = 85%, r_{inter} = 60% and p_{inter} = 10%. As these values resulted in a K_{AC} variability that tended towards the random strand assignment K_{AC} variability (see Fig. 12), parameter re-calibration was required.

To calibrate the strand swapping variables, a three-level Full-Factorial (FF) design was defined, with a focus on reducing the magnitude of strand swaps occurring. This resulted in

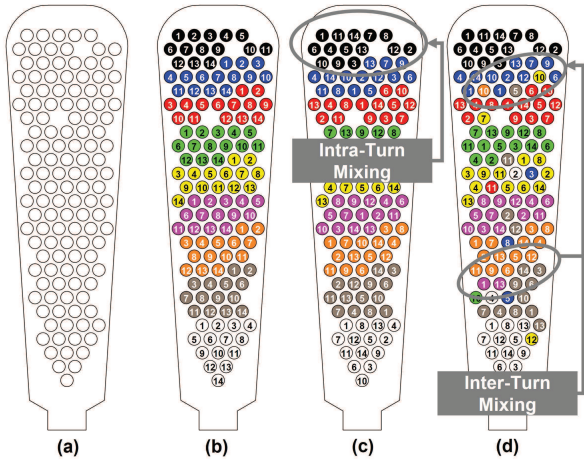

Fig. 13. The statistical simulation process: (a) A simulated conductor lay, (b) the initially assumed tangential strand assignment, (c) intra-turn strand swapping and (d) inter-turn strand swapping

FF levels of: r_{intra} = [5%, 10%, 20%], p_{intra} = [25%, 50%, 75%], r_{inter} = [40%, 50%, 60%] and p_{inter} = [5%, 10%, 15%]. A 100 iteration MCS was performed for each of the 81 parameter combinations. Fig. 14 shows examples of two of the generated $K_{AC} - \delta_{LN}$ distributions.

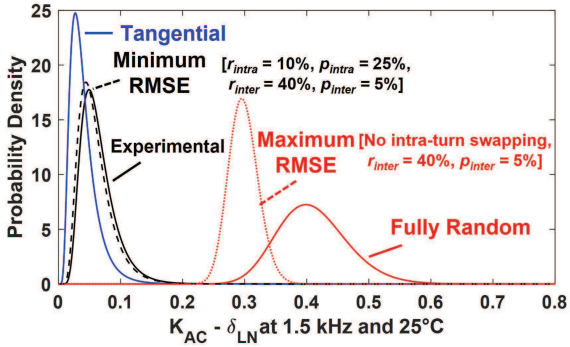

Fig. 14. Selection of the statistical simulation methodology parameters that minimised the error between the generated $K_{AC} - \delta_{LN}$ distribution and the experimentally derived $K_{AC} - \delta_{LN}$ distribution

The values for r_{intra}, p_{intra}, r_{inter} and p_{inter} were selected by identifying the FF design point that minimised the difference between the experimental and statistically simulated $K_{AC} - \delta_{LN}$ distribution using the Root Mean Square Error (RMSE), which was minimised when r_{intra} = 10%, p_{intra} = 25%, r_{inter} = 40% and p_{inter} = 5%, as shown in Fig. 14. Example generated conductor lays are shown in Fig. 15, and it can be seen that the selected parameters resulted in the strands of a series turn remaining grouped (with strand assignment varying within a turn), whilst some individual strands are observed to deviate significantly from their original series turn.

Finally, Fig. 14 also shows the FF point that resulted in the greatest deviation from the experimental $K_{AC} - \delta_{LN}$ distribution. Of note is that this FF point represented no intra-turn mixing, but the same inter-turn mixing levels. Consequently, the importance of accounting for both intra-turn and inter-turn strand mixing has been highlighted.

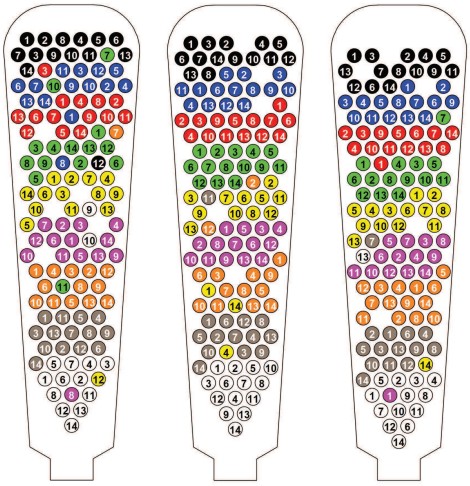

Fig. 15. Example conductor lays and strand assignments from the statistical simulation methodology

D. Validation of Simulation Approach

A further 10,000 iteration MCS was performed at f = 1.5 kHz and T = 25°C for validation. From Fig. 16, it can be observed that the SSM K_{AC} variability lies in between the tangential and fully random strand assignments.

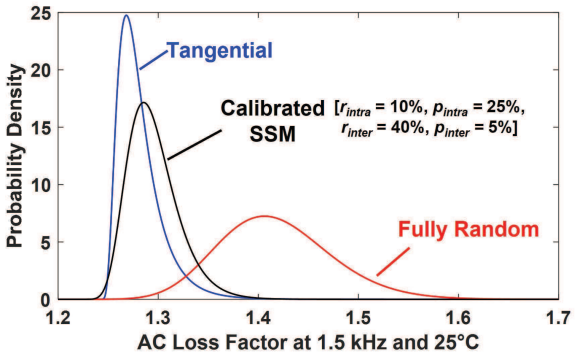

Fig. 16. Monte Carlo Simulation estimates of AC loss variability for the tangential and random strand assignments along with the calibrated statistical simulation methodology

Additional 100 iteration MCSs were performed using the calibrated SSM, at the frequency and temperature test points defined during the experimental AC loss testing. Fig. 17a shows the resulting mean K_{AC} values at each test point, which mirrors the mean K_{AC} trends with respect to frequency and temperature shown for the experimental data in Fig. 3. As observed in Fig. 17b, the variability in K_{AC} increases with increasing frequency. On the other hand, Fig. 17c demonstrates that at a constant frequency, the variability in K_{AC} decreases with increasing temperature. As a result, the calibrated SSM approach is consistent with the experimental trends in AC loss variability.

V. Discussion

To develop recommendations on the future utilisation and development of the analytical and SSM AC loss variability estimation approaches, their $K_{AC} - \delta_{LN}$ distributions for 1.5 kHz at both 25°C and 125°C were compared to the experimental $K_{AC} - \delta_{LN}$ distribution, as performed during SSM calibration in Fig. 14. These distributions are shown respectively in Fig. 18a and 18b and deviation away from the experimental $K_{AC} - \delta_{LN}$ distribution infers a reduced representation of the AC loss variability from a given model.

Firstly, Fig. 18 shows that the analytical model provides a reduced fit to the observed AC loss variability when compared to the SSM at 25°C and 125°C. This is to be expected due to the simplifications present within the analytical approach, when compared to the SSM simulation of conductor positions. The reduced agreement between the analytical model and experimental results at 25°C is also expected to be due to the challenges of achieving thermal steady state during near-ambient testing. Further validation of the analytical model could be performed through reducing the held environmental chamber temperature (providing condensation does not form), and using coil current heating to bring the winding to 25°C.

Fig. 18b also shows that the SSM predicted AC loss variability deviates from the experimental $K_{AC} - \delta_{LN}$ distribution at 125°C as shown in Fig. 18b. One route that could be adopted to enhance the representation of AC loss variability at higher temperatures within the SSM is to calibrate the SSM at multiple operating frequencies and temperatures. As the available stators consisted of thicker laminations than those considered by Thomas et al. [19], there is the potential for higher core losses to be present, leading to disagreement between the FEA and the experimental results.

It is important to note that the analytical model was shown to embody the AC loss magnitude and variability trends observed during experimental testing and provided a good fit to the mean AC loss and the AC loss variability as given by the percentile values shown in Fig. 8. From the results presented in this paper, it is clear that the analytical method is able to estimate the statistical limits often required within engineering design (i.e. 5th and 95th percentile), but does not adequately capture the full shape characteristics of the AC loss variability from Fig. 18. Consequently, the analytical model should be employed to predict AC loss variability at early winding design stages, prior to using the computationally expensive SSM. Currently, the analytical model represents an approach which has been calibrated to fit experimental data. Ongoing work by the authors is conducting AC loss testing of different electric vehicle traction motors of various winding configurations. On the completion of this testing the analytical model will be refitted, to build trends between the AC loss variability model parameters and winding configuration parameters.

The SSM naturally provides a route to capture the specific winding configuration under design and therefore should be adopted during a detailed design phase. The SSM has also captured the lay characteristics that can be inferred from the manufacturing process. As described in Section I, coils consisting of series turns of the parallel strands are formed prior to insertion into the stator slot. Consequently, it would be expected that the slot strand assignment will broadly group the parallel strands of a given series turn. However, coil insertion will disrupt the assignment from a tangential arrangement and

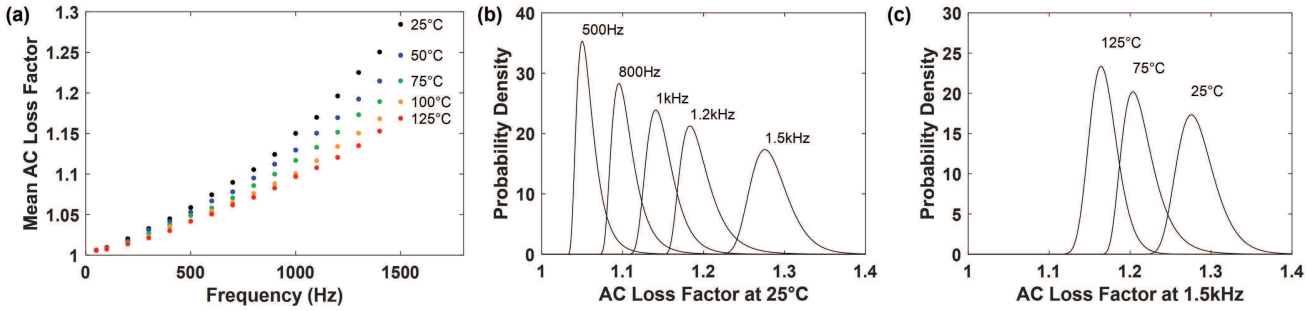

Fig. 17. (a) Mean AC loss values as estimated by the statistical simulation methodology with variation in AC loss variability as estimated by the statistical simulation methodology for (b) various frequencies at 25°C and (c) various temperatures at 1.5 kHz

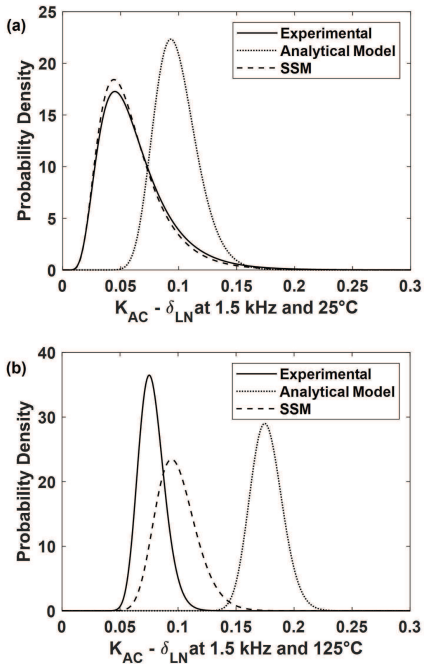

Fig. 18. Comparison of the predicted AC loss variability for the analytical and statistical simulation methods to that observed during experimental testing at 1.5 kHz and (a) 25°C and (b) 125°C

some strands will deviate significantly away from their original turns [13], as also observed in the SSM strand assignments shown in Fig. 15. Ongoing work also aims to facilitate a transition away from a fixed-grid conductor lay, based on the real conductor lays identified by the authors [13] and to develop relationships between intra- and inter-turn mixing and the winding configurations of as-manufactured traction motors.

Finally, Golovanov et al. have detailed an analytical method that accounts for differing conductor location and shape within the slot [50]. Such an approach could reduce the SSM computational expense if coupled with the conductor lay simulation.

VI. Conclusion

The adoption of volume manufactured power-dense electrical machines within the automotive sector has initiated the need to develop design tools to characterise the AC loss magnitude and variability in multistrand stator windings. To date, analytical and finite element analysis approaches have been reliant on assumed conductor lays, leading to deterministic and potentially un-conservative estimates of AC losses in stator windings, which could lead to reduced machine reliability.

This paper has presented two differing approaches to AC loss variability estimation in multistrand stator windings, through adopting analytical and finite element approaches and comparing their behaviour to AC loss variability characteristics observed during experimental testing. The presented finite element analysis approach replicates the conductor lay characteristics observed within previous investigations, whilst the analytical model combines both strand and bundle level AC loss models. Whilst both approaches capture the AC loss variability trends with frequency and temperature, it is recommended that the analytical model should be adopted for early design phases, transferring to the finite element approach once the final winding configuration is known. Ongoing work aims to establish the trends between model parameters and differing winding configurations and manufacturing methods.

References

[1] J. Liu, X. Fan, D. Li, R. Qu, and H. Fang, "Minimization of AC Copper Loss in Permanent Magnet Machines by Transposed Coil Connection," IEEE Trans. Ind. Appl., vol. 57, no. 3, pp. 2460–2470, 2021.

[2] I. Husain, et al., "Electric Drive Technology Trends, Challenges and Opportunities for Future Electric Vehicles," Proc. IEEE, vol. 109, no. 6, pp. 1039–1059, 2021.

[3] A. Bardalai, et al., "Reduction of Winding AC Losses by Accurate Conductor Placement in High Frequency Electrical Machines," IEEE Trans. Ind. Appl., vol. 56, no. 1, pp. 183–193, 2020.

[4] A. Lehikoinen, N. Chiodetto, E. Lantto, A. Arkkio, and A. Belahcen, "Monte Carlo Analysis of Circulating Currents in Random-Wound Electrical Machines," IEEE Trans. Magn., vol. 52, no. 8, pp. 1–12, 2016.

[5] A. Fatemi, D. M. Ionel, N. A. O. Demerdash, D. A. Staton, R. Wrobel, and Y. C. Chong, "Computationally Efficient Strand Eddy Current Loss Calculation in Electric Machines," IEEE Trans. Ind, Appl., vol. 55, no. 4, pp. 3479–3489, 2019.

[6] J. Hagedorn, F. Sell-Le Blanc, and J. Fleischer, Handbook of Coil Winding, Springer, 2018.

[7] J. Fleischer, S. Haag, and J. Hofmann, Quo Vadis Winding Technology? - A study on the state of the art and research on future trends in automotive engineering, Institute of Production Science, 2017.

[8] J. Hofmann, F. Sell-Le Blanc, M. Krause, F. Wirth, and J. Fleischer, "Simulation of the assembly process of the insert technique for distributed windings," 2016 6th International Electric Drives Production Conference (EDPC), pp. 144–148, 2016.

[9] I. Petrov, M. Polikarpova, P. Ponomarev, P. Lindh, and J. Pyrhönen, "Investigation of additional AC losses in tooth-coil winding PMSM with high electrical frequency," XXII International Conference on Electrical Machines (ICEM), pp. 1841–1846, 2016.

[10] D. Bauer, P. Mamuschkin, H. Reuss, and E. Nolle, "Influence of parallel wire placement on the AC copper losses in electrical machines," 2015 IEEE International Electric Machines & Drives Conference (IEMDC), pp. 1247–1253, 2015.

[11] F. Birnkammer, J. Chen, D. Bachinski, and D. Gerling, "Influence of the Modeling Depth and Voltage Level on the AC Losses in Parallel Conductors of a Permanent Magnet Synchronous Machine," IEEE Trans. Appl. Supercond., vol. 28, no. 3, pp. 1–5, 2018.

[12] J. Hoole, P. H. Mellor, N. Simpson, and D. North, "Statistical Simulation of Conductor Lay and AC Losses in Multi-Strand Stator Windings," 2021 IEEE International Electric Machines & Drives Conference (IEMDC), 2021.

[13] J. Hoole, N. Simpson, P. H. Mellor, and A. Daanoune, "Experimental Determination of Conductor Lay and Impact on AC Loss in Volume Manufactured Machines using X-Ray Computed Tomography," 2021 IEEE Energy Conversion Congress and Exposition (ECCE), pp. 3873–3880, 2021.

[14] E. Preci, et al. "Experimental Statistical Method Predicting AC Losses on Random Windings and PWM Effect Evaluation," IEEE Trans. Energy Convers., vol. 36, no. 3, pp. 2287–2296, 2021.

[15] P. Mellor, J. Hoole, and N. Simpson, "Computationally efficient prediction of statistical variance in the AC losses of multi-stranded windings," 2021 IEEE Energy Conversion Congress and Exposition (ECCE), pp. 3887–3894, 2021.

[16] A. Hoffmann, B. Knebusch, J. O. Stockbrügger, J. Dittmann, and B. Ponick, "High-Frequency Analysis of Electrical Machines Using Probability Density Functions for an Automated Conductor Placement of Random-Wound Windings," 2021 IEEE International Electric Machines & Drives Conference (IEMDC), 2021.

[17] P. B. Reddy, and T. M. Jahns, "Analysis of bundle losses in high speed machines," 2010 International Power Electronics Conference - ECCE ASIA -, pp. 2181–2188, 2010.

[18] M. Popescu, and D. G. Dorrell, "Proximity Losses in the Windings of High Speed Brushless Permanent Magnet AC Motors with Single Tooth Windings and Parallel Paths," IEEE Trans. Magn., vol. 49, no. 7, pp. 3913–3916, 2013.

[19] R. Thomas, H. Husson, L. Garbuio, and L. Gerbaud, "Comparative study of the Tesla Model S and Audi e-Tron Induction Motors," 17th Conference on Electrical Machines, Drives and Power Systems (ELMA), 2021.

[20] M. Popescu, and N. Riviere, "Electrical Steel and Motors performances, Role of Lamination Thickness", 9th International Conference on Magnetism and Metallurgy (WMM20), 2020.

[21] A. Młot, M. Korkosz, P. Grodzki, and M. Łukaniszyn, "Analysis of the proximity and skin effects on copper loss in a stator core," Arch. Electr. Eng., vol. 63, no. 2, pp. 211–225, 2014.

[22] R. Wrobel, N. Simpson, P. H. Mellor, J. Goss, and D. A. Staton, "Design of a Brushless PM Starter Generator for Low-Cost Manufacture and a High-Aspect-Ratio Mechanical Space Envelope," IEEE Trans. Ind. Appl., vol. 53, no. 2, pp. 1038–1048, 2017.

[23] P. Mellor, R. Wrobel, D. Salt, and A. Griffo, "Experimental and analytical determination of proximity losses in a high-speed PM machine," 2013 IEEE Energy Conversion Congress and Exposition (ECCE), pp. 3504–3511, 2013.

[24] R. Wrobel, D. E. Salt, A. Griffo, N. Simpson, and P. H. Mellor, "Derivation and Scaling of AC Copper Loss in Thermal Modeling of Electrical Machines," IEEE Trans. Ind. Appl., vol. 61, no. 8, pp. 4412–4420, 2014.

[25] D. North, N. Simpson, and P. Mellor, "Identifying AC Loss Distributions in Electrical Machines through Experimentally Informed Virtual Prototyping," 2020 IEEE Energy Conversion Congress and Exposition (ECCE), pp. 3642–3648, 2020.

[26] C. Roth, F. Birnkammer, and D. Gerling, "Analytical Model for AC Loss Calculation Applied to Parallel Conductors in Electrical Machines," XIII International Conference on Electrical Machines (ICEM), pp. 1088–1094, 2018.

[27] P. B. Reddy, Z. Q. Zhu, S. Han, and T. M. Jahns, "Strand-level proximity losses in PM machines designed for high-speed operation," 2008 18th International Conference on Electrical Machines, 2008.

[28] D. Golovanov, and C. Gerada, "Analytical Methodology for Modelling of Circulating Current Loss in Synchronous Electrical Machines With Permanent Magnets," IEEE Trans. Energy Convers., vol. 37, no. 1, pp. 220–231, 2022.

[29] C. R. Sullivan, "Computationally efficient winding loss calculation with multiple windings, arbitrary waveforms, and two-dimensional or three-dimensional field geometry", IEEE Trans. Power Electron., vol. 16, no. 1, pp. 142–150, 2001.

[30] G. Volpe, M. Popescue, F. Marignetti, and J. Goss, "AC Winding Losses in Automotive Traction E-Machines: A New Hybrid Calculation Method," 2019 IEEE International Electric Machines & Drives Conference (IEMDC), pp. 2115–2119, 2019.

[31] A. Al-Timimy, P. Giangrande, M. Degano, M. Galea, and C. Gerada, "Investigation of AC Copper and Iron Losses in High-Speed Power-Density PMSM," XIII international Conference on Electrical Machines (ICEM), pp. 263–269, 2018.

[32] N. Taran, D. M. Ionel, V. Rallabandi, G. Heins, and D. Patterson, "An Overview of Methods and a New Three-Dimensional FEA and Analytical Hybrid Technique for Calculating AC Winding Losses in PM Machines," IEEE Trans. Ind. Appl., vol. 57, no. 1, pp. 352–362, 2021.

[33] R. Wrobel, A. Młot, and P. H. Mellor, "Investigation of end-winding proximity losses in electromagnetic devices," XIX International Conference on Electrical Machines - ICEM 2010, 2010.

[34] A. Młot, M. Łukaniszyn, and M. Korkosz, "Influence of end-winding size on proximity losses in a high-speed PM synchronous motor," 2015 Selected Problems of Electrical Engineering and Electronics (WZEE), 2015.

[35] D. Winterborne, S. Jordan, L. Sjöberg, and G. Atkinson, "Estimation of AC copper loss in electrical machine windings with consideration of end effects," 2020 International Conference on Electrical Machines (ICEM), pp. 847–853, 2020.

[36] F. Chai, Z. Li, and Y. Yu, "Analysis of AC Losses in High-Speed Permanent Magnet Motors Based on the Equivalent Modeling Method," XIII International Conference on Electrical Machines (ICEM), pp. 1061–1066, 2018.

[37] X. Chen, H. Fang, D. Li, R. Qu, X. Fan, and H. Hu, "Suppression of Winding AC Losses in high-Speed Permanent Magnet Machines by Novel Transposition Technologies," 2021 IEEE Energy Conversion Congress and Exposition (ECCE), pp. 4539–4545, 2021.

[38] M. Kimiabeigi, and J. D. Widmer, "On winding design of high performance ferrite motor for traction application," 2016 XXII International Conference on Electrical Machines (ICEM), pp. 1949–1956, 2016.

[39] M. van der Geest, H. Polinder, J. A. Ferreira, and D. Zeilstra, "Current Sharing Analysis of Parallel Strands in Low-Voltage High-Speed Machines," IEEE Trans. Ind. Appl., vol. 61, no. 6, pp. 3064–3070, 2014.

[40] G. Volpe, M. Popescue, F. Marignetti, and J. Goss, "Modelling AC Winding Losses in a PMSM with High Frequency and Torque Density," 2018 IEEE Energy Conversion Congress and Exposition (ECCE), pp. 2300-2305, 2018.

[41] Y. Xie, J. Zhang, F. Leonardo, A. R. Munoz, M. W. Degner, and F. Liang, "Modelling and Verification of Electrical Stress in Inverter-Driven Electric Machine Windings," in IEEE Trans. Ind. Appl., vol. 55, no. 6, pp. 5818–5829, 2019.

[42] J. Barta, N. Uzhegov, L. Knebl, and C. Ondrusek, "Effect of Additional Copper Losses on the High-speed Induction Machine Performance," XIII International Conference on Electrical Machines (ICEM), pp. 1163–1168, 2018.

[43] X. Fan, D. Li, R. Qu., C. Wang and C. Chen, "Effect of AC losses on temperature rise distribution in concentrated windings of permanent magnet synchronous machines with parallel strands," 20th International Conference on Electrical Machines and Systems (ICEMS), 2017.

[44] K. Yamazaki, T. Furuhashi, H. Yui, H. Ohguchi, S. Imamori, and M. Shuto, "Analysis and Reduction of Circulating Current Loss of Armature Wires in Permanent Magnet Synchronous Machines," IEEE Trans. Ind. Appl., vol. 55, no. 6, pp. 5888–5896, 2019.

[45] A. Lehikoinen, N. Chiodetto, A. Arkkio, and A. Belahcen, "Improved sampling algorithm for stochastic modelling of random-wound electrical machines," J. Eng., vol. 2019, no. 17, pp. 3976–3980, 2019.

[46] C. Du-Bar, and O. Wallmark, "Eddy Current Losses in a Hairpin Winding for an Automotive Application," 2018 XIII International Conference on Electrical Machines (ICEM), pp. 710–716, 2018.

[47] L. Veg, J. Kaska, M. Skalický, and R. Pechánek, "A Complex Study of Stator Tooth-Coil Winding Thermal Models for PM Synchronous Motors Used in Electric Vehicle Applications," Energies, vol. 14, no. 9, 2021.

[48] A. Hoffmann, and B. Ponick, "Statistical Deviation of High-Frequency Lumped Model Parameters for Stator Windings in Three-Phase Electrical Machines," 2020 International Symposium on Power Electronics, Electrical Drives, Automation and Motion (SPEEDAM), pp. 85-90, 2020.

[49] Y. Guo, J. Soulard, and D. Greenwood, "Challenges in Electric Machine Stator Manufacturing and Their Influences on Thermal Performance," 9th International Electric Drives Production Conference (EDPC), 2019.

[50] D. Golovanov, A. Galassini, T. Transi, and C. Gerada, "Analytical Methodology for Eddy Current Loss Simulation in Armature Windings of Synchronous Electrical Machines with Permanent Magnets," IEEE Trans. Ind. Electron., vol. 69, no. 10, pp. 9761-9770, 2022.